Functionally independent components of early event-related potentials in a visual spatial attention task

Scott Makeig[1*], **Marissa Westerfield**[2,3], **Jeanne Townsend**[2,4], **Tzyy-Ping Jung**[3,4,5], **Eric Courchesne**[2,4] **and Terrence J. Sejnowski**[3,4,5,6]

[1]*Naval Health Research Center, PO Box 85122, San Diego, CA 92186-5122, USA (scott@salk.edu)*
[2]*Children's Hospital Research Center, San Diego, CA 92123, USA*
[3]*Institute for Neural Computation, University of California at San Diego, La Jolla, CA 92093, USA*
[4]*University of California at San Diego, La Jolla, CA 92093, USA*
[5]*Computational Neurobiology Laboratory, and* [6]*Howard Hughes Medical Institute, The Salk Institute for Biological Studies,
10100 N. Torrey Pines Road, La Jolla, CA 92037, USA*

Spatial visual attention modulates the first negative-going deflection in the human averaged event-related potential (ERP) in response to visual target and non-target stimuli (the N1 complex). Here we demonstrate a decomposition of N1 into functionally independent subcomponents with functionally distinct relations to task and stimulus conditions. ERPs were collected from 20 subjects in response to visual target and non-target stimuli presented at five attended and non-attended screen locations. Independent component analysis, a new method for blind source separation, was trained simultaneously on 500 ms grand average responses from all 25 stimulus–attention conditions and decomposed the non-target N1 complexes into five spatially fixed, temporally independent and physiologically plausible components. Activity of an early, laterally symmetrical component pair (Nla_R and Nla_L) was evoked by the left and right visual field stimuli, respectively. Component Nla_R peaked *ca.* 9 ms earlier than Nla_L. Central stimuli evoked both components with the same peak latency difference, producing a bilateral scalp distribution. The amplitudes of these components were not reliably augmented by spatial attention. Stimuli in the right visual field evoked activity in a spatio-temporally overlapping bilateral component (N1b) that peaked at *ca.* 180 ms and was strongly enhanced by attention. Stimuli presented at unattended locations evoked a fourth component (P2a) peaking near 240 ms. A fifth component (P3f) was evoked only by targets presented in either visual field. The distinct response patterns of these components across the array of stimulus and attention conditions suggest that they reflect activity in functionally independent brain systems involved in processing attended and unattended visuospatial events.

Keywords: EEG; visual; event-related potential; spatial; attention; independent component analysis

1. INTRODUCTION

Early event-related potentials (ERPs) time locked to abrupt visual stimulus onsets are dominated by a vertex-negative potential deflection, often called N1, occurring from *ca.* 140 to 230 ms after the onset of the visual stimulus. A prominent negative response peak with a similar latency, also called N1 but with a different scalp distribution, is evoked by auditory stimuli. However, neither the auditory nor the visual N1 responses are unitary (Naatanen & Picton 1987). In particular, visual N1 peak amplitude and latency are affected by both stimulus and task variables, including response cueing and attention to location or movement (Mangun & Hillyard 1991; O'Donnell *et al.* 1997; Kotchoubey *et al.* 1997; Valdes-Sosa *et al.* 1998).

An assumption implicit in most ERP research is that coherent neural activations producing ERP components occur in spatially stable and restricted brain regions during information processing. This assumption is consistent with anatomical studies that separate the visual cortex into discrete, interconnected regions, and with the spatially restricted activations typically observed in functional magnetic resonance imaging experiments. However, volume-conducted projections of spatially stable neural generators with overlapping time-courses and scalp projections can produce the appearance of a single ERP peak having a moving distribution on the scalp. In this case, the separate projections can be called either components or subcomponents of the observed peak.

The scalp distribution of N1 typically changes smoothly during its time-course. Because of this, it is suspected that the N1 arises from activity in multiple brain systems (Neville & Lawson 1987). However, decomposing the

*Author for correspondence.

observed responses into subcomponents has not yet been accomplished. ERP components are usually identified with single response peaks in single channel waveforms. By this procedure, for example, Hillyard & Anllo-Vento (1998) and earlier researchers identified an early and a late phase of the N1 complex. However, peak-based methods cannot be used to separate components if they do not produce separate peaks. In addition, spatial stationarity of the responses near a peak of interest is required to ensure that the peak is composed of only one spatially stable component.

Here we apply independent component analysis (ICA) (Bell & Sejnowski 1995; Makeig *et al.* 1996, 1997, 1999), a new approach to the linear multivariate decomposition of multichannel data, to 31-channel recordings during a visual selective attention task (Townsend & Courchesne 1994; Courchesne *et al.* 1990). ICA decomposes ERP data into the sums of brief activations compatible with information processing in a small number of brain networks whose spatial projections to the scalp are fixed across time and task conditions. We hypothesized that data from this five-location selective-attention task might be better suited than simpler task paradigms to the decomposition of early visual components by ICA because this task involved a relatively large number of target and non-target response categories.

Most ERP studies of selective attention have analysed responses to targets and to non-targets separately, because otherwise measures of early stimulus-related components of target responses might be confounded by overlapping early portions of later response-related components (see, for example, Anllo-Vento & Hillyard 1996). The ICA method, however, might allow the time-courses and scalp maps of these components to be identified separately in both target and non-target responses simultaneously. For this reason, we applied ICA to data from all 25 target and non-target conditions. Results suggests that visual evoked activity during the time-course of the visual N1 in these experiments summed at least five functionally independent, spatially stable components with distinct time-courses, scalp maps and relations to the stimulus and task conditions.

2. MATERIALS AND METHODS

(a) *Task design*

Event-related brain potentials (ERPs) were recorded from subjects who attended to randomized sequences of filled round disks appearing briefly inside one of five empty squares that were constantly displayed 0.8 cm above a central fixation cross. The 1.6 cm square outlines were displayed on a black background at horizontal visual angles of $0°$, $\pm 2.7°$ and $\pm 5.5°$ from fixation. During each 76 s block of trials, one of the five outlines was coloured green and the other four blue. The green square marked the location to be attended. This location was counterbalanced across blocks. One hundred single stimuli (filled white circles) were displayed for 117 ms within one of the five empty squares in a pseudo-random sequence with inter-stimulus intervals of 250–1000 ms (in four equiprobable 250 ms steps).

Twenty right-handed volunteers (6 women, 14 men; ages 16–54 years) with normal vision or vision corrected to normal participated in the experiment. Subjects were instructed to maintain fixation on the central cross while responding only to
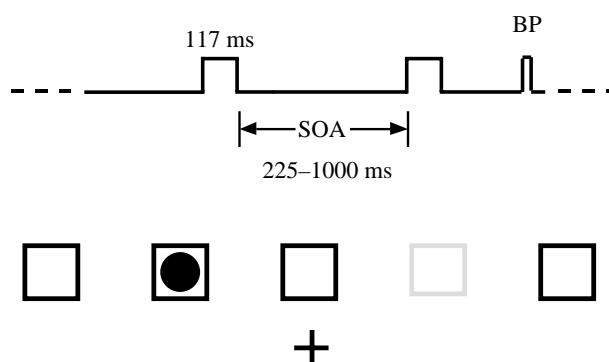

Figure 1. Schematic time line and stimulus display for the experiment. Subjects fixated the screen centre (cross, lower row) while five boxes were displayed continuously above the fixation point. During each 76 s block of trials, one of the boxes was coloured differently from the others, indicating that it was the attended stimulus location for that block. Visual stimuli (single solid disks, duration 117 ms) were displayed briefly in boxes 1 (leftmost) to 5 (rightmost) in pseudo-random order at inter-stimulus intervals of 225–1000 ms. Subjects were asked to press a right thumb button as soon as possible whenever a disk was presented in the attended location.

stimuli (filled circles) presented in the green (attended) square. Subjects were required to press a right-hand-held thumb button as soon as possible after stimuli had been presented in the attended location. Thirty blocks of trials were collected from each subject, yielding 120 target and 480 non-target trials at each location. Subjects were given 1-min breaks between blocks.

(b) *Evoked responses*

Electroencephalogram (EEG) data were collected from 29 scalp electrodes mounted in a standard electrode cap (Electrocap) at locations based on a modified International 10-20 System, and from two periocular electrodes placed below the right eye and at the left outer canthus. All electrodes were referenced to the right mastoid with an input impedance of less than $5\,k\Omega$. Data were sampled at 256 or 512 Hz within an analogue pass band of 0.01–50 Hz. All data were converted digitally to a 256 Hz sampling rate to minimize processing time. To minimize line noise artefacts further, responses were digitally low-pass filtered below 40 Hz before analysis. After rejecting trials containing electro-oculographic potentials larger than $70\,\mu V$, 500 ms (-100–400 ms) brain responses to stimuli presented at each location in each attention condition were averaged separately by using the ERPSS software package (Hansen 1993), producing a total of 25 128-point ERPs for each subject. Responses to target stimuli were considered correct and averaged only when subjects responded between 150 and 1000 ms. No responses shorter than 200 ms were noted. Data averages studied in this report are available at http://www.cnl.salk.edu/~scott/20ssnl.txt.gz.

(c) *ICA*

The ICA algorithm we used in this study (Bell & Sejnowski 1995, 1996; Lee *et al.* 1999a) is an 'infomax' neural network (Linsker 1992; Nadal & Parga 1994) that uses stochastic gradient ascent to find a square 'unmixing' matrix that maximizes the joint entropy (Cover & Thomas 1991) of a nonlinearly transformed ensemble of zero-mean input vectors. Infomax ICA is one of a family of algorithms that exploit

temporal independence to perform the blind separation of linear mixtures of source signals. Recently, Lee *et al.* (1999*a*) have shown that these algorithms have a common information-theory basis, differing chiefly in the form of source distribution, which might not be critical (Amari 1998). Logistic infomax can accurately decompose mixtures of component processes having symmetrical or skewed distributions, even without using non-linearities specifically tailored to them.

At the end of training, multiplying the input data by the output (or 'unmixing') weight matrix gives a data matrix whose rows, called the component activations, give the time-course of the relative strength or activity level of the respective independent components across conditions. ICA component activations are similar to the 'factor weights' produced by spatial principal component analysis (PCA). The columns of the inverse of the weight matrix give the relative projection strengths of the respective components onto each of the scalp sensors. These can be interpolated to show the 'scalp map' associated with each component. ICA scalp map weights are similar to spatial eigenvectors or 'factor loadings' produced by spatial PCA.

Unlike components produced by PCA, however, component scalp maps returned by ICA are not constrained to be orthogonal and are therefore free to reflect accurately the actual overlapping projections of functionally separate sources, if and when ICA successfully separates them. PCA is useful primarily for dimension reduction, but is less likely to separate data into functionally separate components. For example, Makeig *et al.* (1999) have shown that ICA, applied to these same response epochs (-100 to 900 ms) gave a decomposition of the late positive complex (LPC, or P300) that was more tightly related to behaviour, and better replicated between two subject subgroups, than decompositions based on PCA with or without Varimax or Promax rotation.

The projection of the *i*th component onto the original data channels is given by the outer product of the *i*th column of the inverse weight matrix with the *i*th row of the component activation matrix, and is in the original units (for example microvolts). An overview of the assumptions of the ICA algorithm and their relation to ERP data is available elsewhere (Makeig *et al.* 1999). More information plus a collection of Matlab routines for performing and visualizing the analysis are available on the Web (http://www.cnl.salk.edu/~scott/ica.html).

(d) *Evoked response decomposition*

In general, the independence assumption used by ICA is not known to hold exactly for actual ERP data. In this case very large components, including the LPC in responses to target stimuli in these experiments, might have a disproportionate influence on the decomposition of smaller components. For this reason we selected an analysis time window ending 400 ms after stimulus onset. Trial decompositions of shorter time windows gave very similar results (although differing in some details, as discussed below), but did not include enough of the LPC onset to determine which LPC subcomponents contributed to N1.

The logistic infomax ICA algorithm was applied to sets of 25 ERP averages (31 electrode channels, 128 time points) time-locked from 100 ms before to 400 ms after the onsets of target and non-target stimuli presented at each of the five stimulus locations in the five spatial attention conditions. Decompositions were performed on grand averages of data from all 20 subjects with the use of various time windows. Thus, a total of $5 \times 5 \times 31 = 775$ 500-ms ERP traces were analysed simultaneously. ICA decomposition was performed by using routines

running under Matlab 5.01 on a Dec Alpha 300 MHz processor (Makeig *et al.* 1997, 1999). The learning batch size was 65. The initial learning rate started near 0.004 and was gradually reduced to 10^{-6} during 50–100 training iterations that required *ca.* 5 min of computer time. Results of the analysis were relatively insensitive to the exact choice of learning rate or batch size.

3. RESULTS

Although the appearance of the earliest recognizable visual evoked response peak, P1 (near 140 ms), was highly variable across the 25 response conditions, each contained a negative-going N1 component peaking at different scalp sites between 165 and 195 ms. The amplitude and duration of the N1 deflection varied considerably between scalp sites across stimulus and attention conditions. In all five target–response conditions, the N1 deflection was followed by P2 and N2 peaks, then an LPC (often called P3 or P300) (Makeig *et al.* 1999).

During the time-course of the N1 response, the scalp topography of the responses changed continuously (figure 2*a*, scalp maps), suggesting the presence of multiple overlapping components. The ICA decomposition of all 25 31-channel ERPs returned 31 components. Figure 2*b* shows the scalp maps of the six largest independent components. These had fixed scalp distributions and independent time patterns of activation across conditions. The largest two accounted for the early and middle phases of the LPC. Two others accounted for the late portion of the N1 and early portion of the P2 peaks, respectively. A third pair of components accounted for the early phase of N1 in all conditions. One of these, which we labelled N1a$_L$, was activated by stimuli presented in the left visual field. The other, labelled N1a$_R$, was activated by stimuli in the right visual field. Stimuli presented in the central location, just above fixation, activated the left and right visual field response components together with nearly equal amplitudes. Components N1b and P2a peaked later than the N1a pair, whose scalp maps were nearly laterally symmetrical. Still later and larger components P3f and P3b were evoked only by target stimuli.

Figure 2*c* illustrates a measure useful for visualizing the relation of component projections to the original data. The envelope of a multichannel data epoch can be defined as a pair of time-series consisting respectively of the most positive value and the most negative value in all or some data channels at each time point. For a given response epoch, the envelopes of the separate projections of each ICA component to the scalp electrodes can be defined similarly. Envelope plots can give useful indications of the latency, predominant polarity and amplitudes of temporally overlapping response and component features. Figure 2*c* shows the grand-mean target response at all 29 scalp channels (blue traces) above its data envelope (black traces).

Figure 2*d* (black traces) shows the envelopes of the grand-mean responses to non-target stimuli presented in the far right, centre and far left locations, respectively, along with the envelopes of components N1a$_R$ and N1a$_L$. The vertical broken lines (at 162 ms) demonstrate that the activations of both components in response to central stimuli peak at the same latencies as in responses to
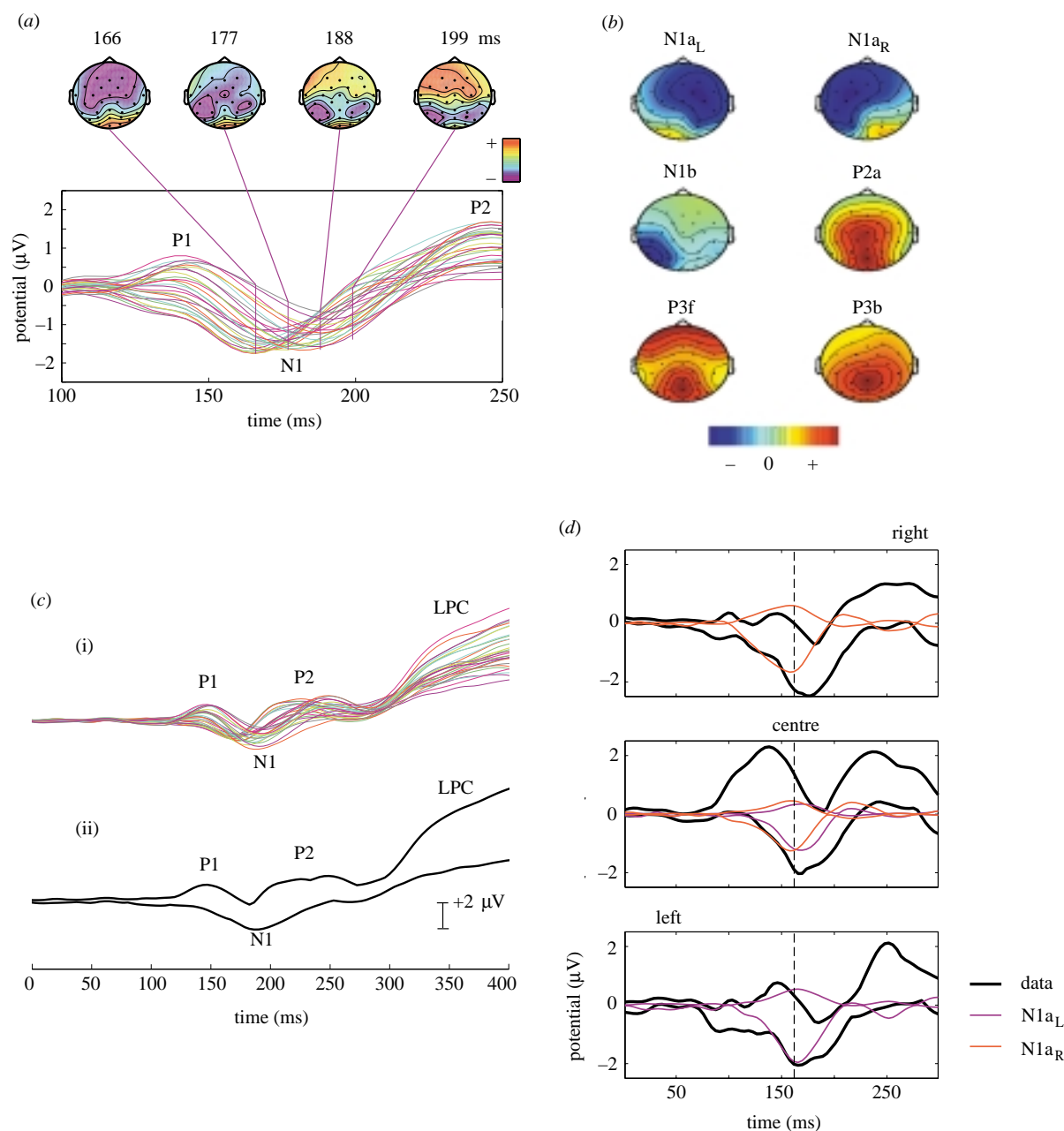
Figure 2. (*a*) The grand-mean response for all 20 non-target conditions and 20 subjects. Responses at all 29 scalp channels are shown on the same baseline. Note that N1 component peak latency differs at each electrode site. The scalp maps illustrate the continuously shifting potential distribution through the N1 peak. The maps have been scaled individually to their minimum and maximum values to highlight shifts in the scalp distribution of the response. (*b*) Scalp maps of the six largest independent components, individually scaled (green represents zero weight). Relative locations of the electrodes are shown by small dots. Colour polarities are chosen to represent the signs at their time point of maximum projection (with red positive and blue negative with respect to the reference). Note the bilateral near-symmetry of the two early-N1 components (top row). (*c*) The upper (blue) traces show the grand-mean target response averaged across all 20 subjects and 5 target conditions at the 29 scalp channels. The time series defined by the most positive and most negative potential values across all channels at each time point can be termed the 'envelope' of the data, as shown in the lower panel (black traces). Conventional peak labels are shown. (i) Target response; (ii) response envelope. (*d*) Envelopes of independent components N1a_L and N1a_R in the grand-mean responses to non-target stimuli presented at far right, central and far left locations, respectively. The vertical broken lines mark 162 ms. Note the stable component peak latencies across conditions, and their *ca.* 9 ms difference. Envelopes were computed across 29 scalp channels.

lateral stimuli in which only one of the pair is active. At some time points, the data envelopes are smaller than the response envelopes. This occurred when the projections of other components (including N1b) had opposite signs at some scalp channels and cancelled the N1a-component projections.

To explore the patterns of activation of each of the components across conditions, the envelopes of each of the six component projections, in all 25 response conditions, were plotted in grid arrays (figure 3). The top pair of grids shows the activations of components N1a_L and N1a_R, respectively. Within each grid, five columns (left to
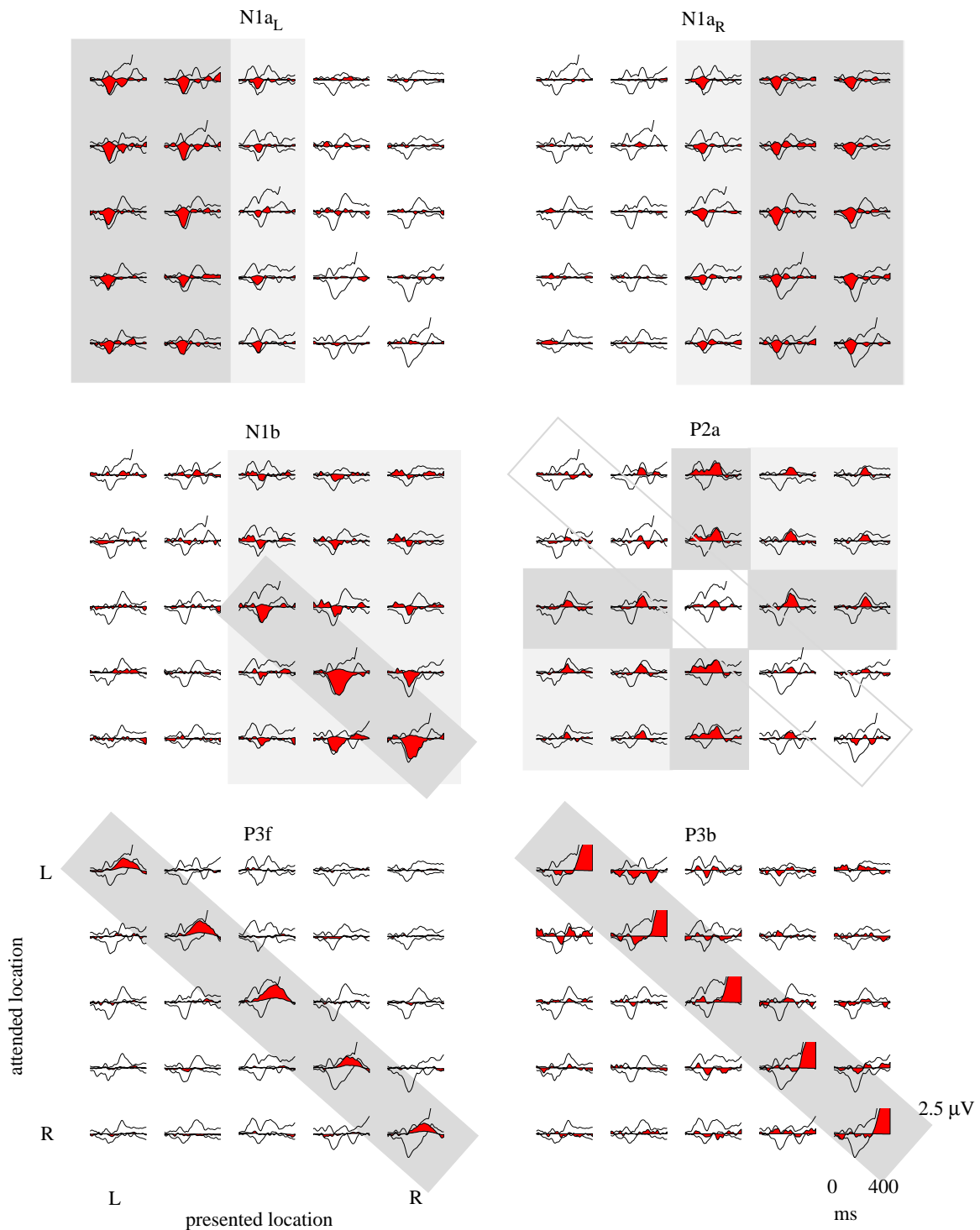
Figure 3. Envelopes of the six largest independent components (black outline, filled with red, from all 29 scalp and two electro-oculographic channels) (compare figure 2*b* above), superimposed on the mean response envelopes for all 25 presented–attended location conditions. Note the systematic differences between the sets of conditions in which the different components are active: N1a$_L$ and N1a$_R$ (top row) are evoked by left and right visual field stimuli, but do not seem to depend in any simple way on the attended location. Both also respond to midline stimuli. N1b (centre left) responds to right visual field stimuli. Its amplitude is enhanced both in attended locations and to a smaller extent in nearby right visual field locations (locations (4,5) and (5,4)). P2a, in contrast (middle right), has little or no response to targets (diagonal traces). Its amplitude is generally largest for non-target midline stimuli. Components P3f (lower left) and P3b (lower right, amplitude clipped) account for overlapping early and middle portions of the LPC (Makeig *et al.* 1999) in responses to target stimuli presented at attended locations.

right) represent responses to stimuli presented at the respective five locations; the five rows (top to bottom) represent responses produced during attention to each of the same five locations. For maximum visibility, the

envelope of the selected component projection is shown as a filled shape superimposed on the total response envelope. The left and right visual field response patterns of N1a$_R$ and N1a$_L$ are evident, as is their concurrent
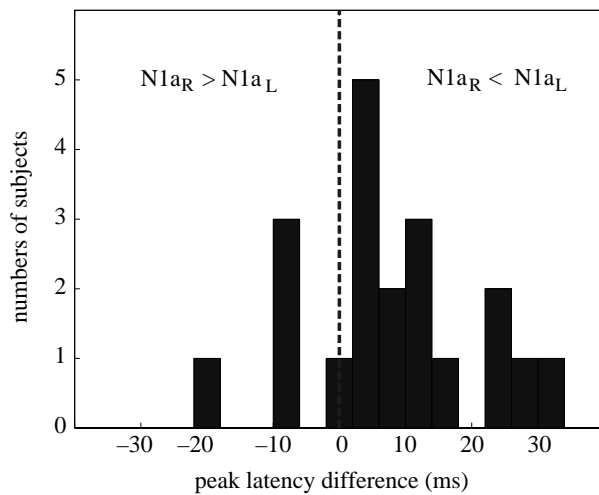
Figure 4. Histogram of peak latency differences between components $N1a_R$ and $N1a_L$ in single subjects. Differences were computed by applying the spatial filters for these two components derived from the grand averages to the 20 single-subject mean responses to left visual field (box 1 or 2) and right visual field (box 4 or 5) stimuli, respectively. Results (significant by *t*-test, $p < 0.02$) compare well with the *ca.* 9 ms ($N1a_R - N1a_L$) latency difference found in the grand average decomposition (figure 2*d*).
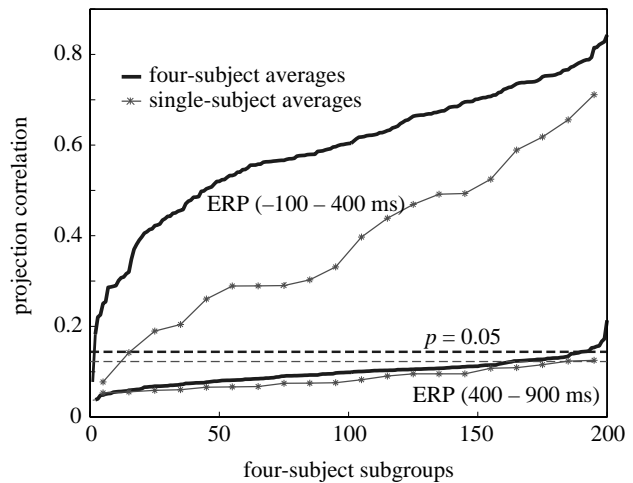

Figure 5. Bootstrap analysis of variability in ICA decompositions from single subjects and subject subgroups. The plot shows rank-ordered correlation coefficients between the time-course in all 25 conditions of component $N1a_R$ (from the grand average decomposition) and (thin traces) the time-course of the most highly correlated independent component derived from separate training on each of the 20 subjects' data, or (thick lines) on averages of data from 200 randomly selected subgroups of four subjects. The top two traces show correlations between ERPs in the time range −100 to 400 ms. As a control, data from a later portion of the same response epochs (400–900 ms after stimulus onset) were used to derive ICA components, and the resulting component projections were correlated with the same grand-mean $N1a_R$ projection (lower traces). Note that nearly all the control correlations fall below the broken lines that give the $p = 0.05$ confidence levels in the single-subject and subject subgroup control data results.

activation after centrally presented stimuli. There was no marked or consistent modulation of component amplitudes by attention. Although an interesting trend appeared in response to central stimuli (a somewhat larger $N1a_R$ amplitude when attention was to the left; a somewhat smaller $N1a_L$ amplitude in response to central targets), we did not at that point test the between-subject reliability of these effects.

The complementary unilateral $N1a_R$ and $N1a_L$ response patterns are clearly shown in figure 3. In response to leftmost stimuli, $N1a_L$ accounted for nearly all of the early phase of the N1, whereas the $N1a_R$ activation was very small and inconsistent. The opposite was true in responses to rightmost stimuli. Here, component $N1a_R$ accounted for the early N1, and $N1a_L$ had only a very small activation. After central stimuli, however, both $N1a_R$ and $N1a_L$ were nearly equally active.

Across all response conditions, the $N1a_R$ peak occurred *ca.* 9 ms before the $N1a_L$ peak (means across the 15 respective active conditions: 157.6 ± 2.7 ms compared with 166.4 ± 3.7 ms). This latency difference was robust across conditions (by *t*-test, $p < 0.000001$). However, group means of the subject median reaction times to targets presented at the five locations had a different U-shaped character, with mean response time to central stimuli *ca.* 10 ms faster than responses to either leftmost or rightmost stimuli.

To test the reliability of the latency difference across subjects, we applied the spatial filters for $N1a_R$ and $N1a_L$ to grand averages of responses to all left visual field (boxes 1 and 2) and right visual field (boxes 4 and 5) stimuli, respectively, from each of the 20 subjects. We then measured the latencies of the largest (frontal-negative) peak in the resulting activation waveforms between 145 and 185 ms. Results, illustrated in figure 4, indicated a

reliable tendency for $N1a_R$ to peak earlier than $N1a_L$ ($p < 0.02$ by *t*-test on the peak latency difference).

The middle pair of grids in figure 3 shows the projections of components N1b and P2a. N1b was evoked nearly exclusively by stimuli presented at the midline and in the right visual field. It was much larger after targets (lower right diagonal) than after non-targets. There was no corresponding left-responding component; N1 in the left visual field conditions was nearly completely accounted for by $N1a_L$ (see upper-left grid). Component P2a, in contrast, was smallest after attended stimuli. It was evoked primarily by stimuli presented in non-attended locations, and particularly by non-attended midline stimuli. Responses to non-targets in the (attend mid-left/ present far-left) and (attend mid-right/present far-right) conditions were also small, possibly reflecting a spatial generalization of response inhibition lateral to a left or right visual field attentional focus.

The bottom row of grids in figure 3 shows the behaviour of the first two of three components recently identified as contributing to the LPC in these data (Makeig *et al.* 1999). Component P3f was evoked exclusively by stimuli presented in the attended location. P3f onset was near 160 ms, after the onsets of all three N1 components and near the $N1a_R$ and $N1a_L$ peaks. A much larger component, P3b (amplitude clipped at $+ 2.5\,\mu V$ in the plot), was also evoked nearly exclusively by target stimuli.

The onset of P3b (near 290 ms) followed the offset of the N1 deflection. Some small, disorganized P3b activation in response to non-target stimuli might represent a 'spillover' of this dominant component into other small and topographically similar data periods owing to insufficient component independence in the ICA training data.

Figure 5 shows the results of bootstrap testing of the reliability of component Nla_R in single-subject decompositions. First, each subject's data (25 500-ms ERP averages) were decomposed by using ICA. Next, the projections of the largest 16 independent components to ten of the scalp channels (chosen at random to save computer resources) were in comparison by using correlation with the projections of Nla_R to the same ten channels in all 25 conditions. These correlations thus involved a comparison of microvolt values at $25 \times 256 \times 10 = 64\,000$ data points representing responses in all 25 stimulus–task conditions.

A second 500 ms time epoch (400–900 ms after stimulus) from the same epochs was used for comparison. Because dominant activity in N1 generators might be assumed to be absent from ERPs beginning more than 400 ms after a visual stimulus onset, these later data sub-epochs gave us an approximate or best available example of averages of spontaneous EEG epochs with the same number of sums as our early response epochs. Figure 5 (thin starred traces) shows the correlations between the projections of the best-fitting independent component (time-courses multiplied by scalp maps) from the single-subject decomposition and the Nla_R in the grand-mean responses. (For the late-epoch components, the ordered absolute values of the correlations are shown.) The two distributions are almost totally disjoint, reflecting the fact that N1-like activity was present in nearly every subject, and that ICA found at least one component of nearly every subject whose response map, time-course and distribution across conditions resembled that of Nla_R. For ten out of the 20 subjects, the best correlation exceeded 0.4, a remarkable result considering that these correlations took into account both the scalp distributions and time-courses of the entire 500 ms responses both within and across conditions.

The thick traces show the results of decomposing averages of all 25 early and late responses, respectively, from 200 random four-subject subgroups. Here the ensembles of best component correlations for the early and late epochs were even more disjoint, and the best-correlated early response component projection was correlated over 0.5 with the Nla_R projection for more than three-quarters of the four-subject averages. Applying the same process to averages of larger subject subgroups might be expected to produce components whose projections were closer and closer to Nla_R.

4. DISCUSSION

(a) *Functional independence of ICA components*

Although the N1 peak in these data contained only one broad positive peak at each scalp channel and condition (as in figure 2a), ICA produced a robust and parsimonious decomposition of electrical activity during the N1 complex into at least five spatially fixed, temporally independent and partly overlapping components (Nla_L, Nla_R, N1b, P2a and P3f). The robustness of the decomposition, the relatively simple and distinct scalp distributions, and

the selective modulation of the amplitudes of these components with the spatial location and the attended location, suggest that they might correspond to functionally distinct brain systems. These results support the conclusions of earlier ERP researchers that the visual N1 response complex is composed of more than one spatially stable component. However, before we can have confidence in the generality of these results, an ICA decomposition of additional experiments with different spatial attention tasks is needed, as well as comparisons of single-subject decompositions of averages and single-trial data.

The problem of comparing group grand-mean response decompositions with ICA decompositions of single-subject responses is a difficult one. Grand-mean data sets have the unique advantage that the strength of background EEG processes that are not time- and phase-locked by experimental events is reduced by a factor generally equal to the square root of the number of subjects. For experiments in which a relatively few trials are collected (for example target trials), this fact might be significant for ICA. Assuming that the number, timing and spatial projections of event-related brain processes (i) common to the group of subjects and (ii) producing appreciable scalp potentials is relatively small, an ICA decomposition of grand-mean responses might have the best chance of recovering accurate evidence of the number, timing and mean scalp projections of the processes. Single-subject averages, in contrast, contain more remnants of background EEG processes, which are moreover superimposed by the averaging process, even if they actually occur in separate trials. The more processes that are summed in relatively brief evoked response epochs, the less chance there is that ICA can separate them cleanly, unless their independence is expressed across the ensemble of evoked responses representing multiple task and response conditions.

We have investigated three approaches to comparing single-subject responses by using ICA. A simple and useful approach (see figure 4) is to apply single-component filters for independent components of the grand average to single-subject response data. Here the grand-mean components are used as measurement tools that combine multiple channels and/or time points in ways that are characteristic of the grand-mean responses. This approach can compare favourably with separate measurements of response peaks at single scalp channels, when these peaks are composed of activity generated by different brain (or non-brain) sources. However, like single-channel peak measures, it can fail to take into account systematic differences in scalp projections and/or time-courses in different subsets of the subjects.

A second approach is to apply separate decompositions to single-subject averages, or to averages of subgroups of subjects, as shown in figure 5. However, results of such comparisons can be difficult to fit into a simple statistical model, because subjects can differ in the strengths, latencies, spectral character and scalp distributions of each of the components found in the grand-mean decomposition. A third approach seeks to reduce the number of overlapping and non-independent EEG processes present in the data at each time point by simply decomposing ensembles of single-trials before any averaging. This approach shows

great promise (Jung *et al.* 1999), but more work is necessary to evaluate its usefulness thoroughly.

(b) P1 decomposition

In these experiments, the first positive visual evoked response peak, P1, appeared only in responses to stimuli presented at midline or, to a smaller extent, in the left visual field. The reason for this response variability is not known. Similar distributions were observed in averages of separate subject subgroups, so the P1 observed here is not an artefact of too few trials. It is possible that the location of the fixation point, slightly below the five stimulated locations, might account for the observed pattern. In the decomposition reported here, no single ICA component accounted for P1. However, a single component accounting for most of the P1 activity did appear in an exploratory decomposition of these same data epochs with the use of a narrower time window (−100 to 250 ms).

This difference between the two decompositions illustrates the statistical and exploratory nature of ICA decomposition, given EEG data for which the ICA assumption of strict independence between source components might not apply precisely. Both ICA decompositions produced a set of multidimensional filters by which relatively independent variations in the data across time and conditions could be observed and measured. The usefulness of these decompositions depends on the degree to which they reveal or highlight functionally independent features in the data, and to the extent to which they generalize across experimental conditions.

(c) Latency difference between N1a_R and N1a_L

The component scalp maps of the $N1a_R$ and $N1a_L$ were broadly distributed and bipolar (figure 2*b*), which is compatible with the assumption that visual evoked response components originating in posterior visual cortex might propagate by volume conduction to EEG electrodes on all parts of the scalp. After their separation by ICA from three other overlapping response components and residual EEG, the activities of these two components were found to account for most or all early N1 activity in all 25 response conditions. In contrast with previous reports that central stimuli produce a bilateral N1 (Neville & Lawson 1987), ICA accounted for the bilateral N1 response to midline stimuli in these experiments as a sum of two lateralized components ($N1a_R$ and $N1a_L$), each of whose 'receptive fields' included midline stimuli.

The stable tendency for component $N1a_R$ to peak *ca.* 9 ms before $N1a_L$ in these data, even in response to midline stimuli, replicates previous reports that right visual field stimuli tend to produce earlier N1 peaks at some scalp sites (Saron & Davidson 1989; Brown *et al.* 1994; Ipata *et al.* 1997). However, those authors measured this latency difference at individual electrode sites, and reported only a complex pattern of latency differences across the scalp. ICA, in contrast, gave nearly the same *ca.* 9 ms difference between the $N1a_R$ and $N1a_L$ peaks after either lateral or midline stimuli.

Previous reports have interpreted N1 latency differences observed at scalp sites ipsilateral and contralateral to the stimulated hemifield as a reflection of the callosal interhemispheric transfer time. ICA, in contrast, modelled the N1 responses observed at each scalp site as weighted sums

of the projected activity of at least five independent components. According to the ICA model, N1 peak latency at each scalp site depended on the relative strength and polarity of the projections of all five ICA components to that site, implying a complex relation between single-electrode peak latencies and those of the underlying components, with little if any direct relation to interhemispheric transfer time. The *ca.* 9 ms early-N1 latency difference provided by ICA, in contrast, was independent of scalp channel, as well as being stable across conditions and subjects (figure 4). However, the origin and function of this difference are unknown.

(d) N1a and attention

To a first approximation, $N1a_R$ and $N1a_L$ were not themselves modulated in any simple manner by visual spatial attention in these experiments (figure 3). The enlarged N1 peaks in responses to right visual field attended stimuli were produced by substantial modulation of N1b by attention (see below); attended left visual field stimuli in these experiments did not evoke an enlarged N1. It might prove revealing to fit the generators of $N1a_R$ and $N1a_L$ scalp distributions with the use of multiple dipole or more general source models.

(e) N1b and attention

In addition to the two early N1a components, ICA identified three later components whose activities began or peaked during the N1 complex under different conditions. Peak activations of these components were all strongly modulated by spatial attention. N1b, a left lateral-posterior negativity, responded to right visual field stimuli only, and much more strongly to targets. There was no homologous late-N1 deflection in the grand-mean responses to left visual field stimuli (figure 3) and therefore no corresponding independent component. The reason for this lateralized response difference is unknown. Several lines of evidence suggest that the right hemisphere is involved in the attentional processing of information from both visual hemifields, whereas the left hemisphere directs attentional responses to information in the right visual field only (Corbetta *et al.* 1993; Heilman *et al.* 1987; Mesulam 1981). Possibly, exclusive left-hemisphere attentional enhancement of attended right visual field stimuli is consistent with the asymmetry of the N1b, and right-hemisphere bilateral attentional control with the somewhat greater right-hemisphere involvement in later components P2a and P3b, which were sensitive to attended locations in either hemifield.

(f) P2a and inattention

P2a, a bilateral positivity largest at precentral and central posterior sites, was evoked primarily in response to non-targets in either hemifield. Its scalp map showed more right-central than left-central scalp activity. Components appearing only in response to stimuli presented in spatially unattended locations have not previously been reported, although it might have been present in previous selective attention responses (see, for example, Anllo-Vento & Hillyard 1996, fig. 3). For this and other components, ICA decomposition revealed a variety of systematic patterns of activation across response conditions that could easily have been missed even by expert observers.

In particular, researchers looking for data features related to spatial attention might not expect to find that stimuli presented at non-attended locations in this experiment had a larger and topographically consistent early P2. Component P2a, however, exhibited this response profile, which was unique among the largest components, making it easy to identify.

The scalp distribution of P2a was anterior to the major target-evoked component, P3b (Makeig *et al.* 1999). Possibly, P2a might be involved in resetting cortex for further processing by adjusting short-term expectancy of target versus non-target. P3b, in contrast, might reflect more widespread brain activity involved in the resetting of both stimulus expectancy and response preparation after target events.

(g) *P3f and rapid responding*

Component P3f had a bilateral frontoparietal scalp distribution, and was evoked only by target stimuli. Results shown in figure 3 replicate our earlier observations, which were based on the decomposition of 1s epochs (−100 to 900 ms) for ten of these subjects, that P3f onset in these experiments occurred near the peak of the N1 complex (Makeig *et al.* 1999). In faster responders among these subjects, P3f peak amplitude occurred very near the moment of the subcortical motor command (Makeig *et al.* 1999). The target-selective nature of P3f, its frontoparietal topography and its close association with response onsets in faster responders all suggest that it might be associated with spatial orientating and motor response engagement. Its scalp distribution seems consistent with the bilateral frontoparietal pattern of haemodynamic activation reported recently by Corbetta *et al.* (1998) during both covert and overt shifts of attention from a central fixation point. Preliminary comparison of data from normal and clinical subjects in this task has suggested that the cerebellum might also have a role in the brain system P3f indexes (Westerfield *et al.* 1998).

In general, the physiological and cognitive functions of the brain systems generating visual evoked response components are unknown. By the time of their onset (all after 100 ms), information about the visual stimulus onset should already have propagated throughout the visual cortex. This suggests that these components might be a reflection of later stages of visual processing rather than the earliest stages, which occur within the first 50 ms in primary visual cortex. One possibility is that N1 and subsequent ERP components (as well as still longer lasting event-related perturbations in the continuing EEG spectrum) are involved in the integration of visual information across successive visual fixations, and/or in preparing cortex to process further visual information (Makeig 1993; Gilbert 1998).

Here we note that ICA can be seen as a very general information-based factor analytical method that can usefully be applied to the analysis of multidimensional data in many contexts. Other promising ICA applications to brain data include analyses of functional magnetic resonance imaging (McKeown *et al.* 1998), single-trial EEG analysis (Makeig *et al.* 1998; Jung *et al.* 1999) and artefact removal (Jung *et al.* 1998), and optical recording data (Brown *et al.* 1998).

(h) *Conclusions*

These results demonstrate that ICA can decompose ERP data sets composed of many scalp channels, stimulus types and task conditions into temporally independent, spatially fixed and physiologically plausible components without necessarily requiring the presence of multiple local response peaks. ICA decomposition provided a parsimonious model of these data that would have been difficult or impossible to build manually from the separate consideration of all 775 single-channel waveforms that were simultaneously analysed by ICA. The N1 components derived by ICA had distinct and simple-appearing scalp distributions. Each accounted for major features of some of the responses, and their patterns of activation covaried in unique but orderly ways with stimulus location and attended location. These findings are consistent with many anatomical and brain imaging studies showing that human cortex contains specialized systems that process various types of visual information, and that activity in many of these areas is enhanced by, or requires, spatial attention. The physiological origins and functions of these new ERP components deserve further analysis.

REFERENCES

Amari, S. 1998 Natural gradient works efficiently in learning. *Neural Comput.* **10**, 251–276.

Anllo-Vento, L. & Hillyard, S. A. 1996 Selective attention to the color and direction of moving stimuli: electrophysiological correlates of hierarchical feature selection. *Percept. Psychophys.* **58**, 191–206.

Bell, A. J. & Sejnowski, T. J. 1995 An information-maximization approach to blind separation and blind deconvolution. *Neural Comput.* **7**, 1129–1159.

Bell, A. J. & Sejnowski, T. J. 1996 Learning the higher-order structure of a natural sound. *Network: Comput. Neural Syst.* **7**, 261–270.

Brown, G. D., Yamada, S., Luebben, H. & Sejnowski, T. J. 1998 Spike sorting and artifact rejection by independent component analysis of optical recordings from tritonia. *Soc. Neurosci. Abstr.* **24**, 1670.

Brown, W. S., Larson, E. B. & Jeeves, M. A. 1994 Directional asymmetries in interhemispheric transmission time: evidence from visual evoked potentials. *Neuropsychologia* **32**, 439–448.

Corbetta, M., Miezin, F. M., Shulman, G. L. & Petersen, S. 1993 A PET study of visuospatial attention. *J. Neurosci.* **13**, 1202–1226.

Corbetta, M. (and 10 others) 1998 A common network of functional areas for attention and eye movements. *Neuron* **21**, 761–773.

Courchesne, E., Akshoomoff, N. A. & Townsend, J. 1990 Recent advances in autism. *Curr. Opin. Pediatr.* **2**, 685–693.

Cover, T. M. & Thomas, J. A. 1991 *Elements of information theory.* New York: Wiley.

Donchin, E. 1966 A multivariate approach to the analysis of average evoked potentials. *IEEE Trans. Biomed. Engng* **13**, 131–139.

Gilbert, C. D. 1998 Adult cortical dynamics. *Physiol. Rev.* **78**, 467–485.

Hansen, J. S. 1993 *Event-related potential software system.* La Jolla: Event-Related Potential Laboratory, University of California San Diego.

Heilman, K. M., Watson, R. T., Valenstein, E. & Goldberg, M. E. 1987 Attention: behavioral and neural mechanisms. In *The handbook of physiology.* 1. *The nervous system* (ed. F. Plum, V. B. Mountcastle & S. T. Geiger), vol. 5, pp. 461–481. Bethesda, MD: American Physiological Association.

Hillyard, S. A. & Anllo-Vento, L. 1998 Event-related brain potentials in the study of visual selective attention. *Proc. Natl Acad. Sci. USA* **95**, 781–787.

Ipata, A., Girelli, M., Miniussi, C. & Marzi, C. A. 1997 Interhemispheric transfer of visual information in humans: the role of different callosal channels. *Arch. Ital. Biol.* **135**, 169–182.

Jung, T.-P., Humphries, C., Lee, T.-W., Makeig, S., McKeown, M., Iragui, V. & Sejnowski, T. J. 1998 Extended ICA removes artifacts from electroencephalographic recordings. In *Advances in neural information processing systems*, vol. 10 (ed. M. M. Kearns, M. Jordan & S. Solla), pp. 894–900. Cambridge, MA: MIT Press.

Jung, T.-P., Makeig, S., Westerfield, M., Townsend, J., Courchesne, E. & Sejnowski, T. J. 1999 Analyzing and visualizing single-trial event-related potentials. In *Advances in neural information processing systems*, vol. 11 (ed. M. S. Kearns, S. A. Solla & D. A. Cohn), pp. 894–900. Cambridge, MA: MIT Press.

Kotchoubey, B., Wascher, E. & Verleger, R. 1997 Shifting attention between global features and small details: an event-related potential study. *Biol. Psychol.* **46**, 25–50.

Lee, T.-W., Girolami, M., Bell, A. J. & Sejnowski, T. J. 1999*a* A unifying framework for independent component analysis. *Int. J. Math. Comput. Models.* (In the press.)

Lee, T.-W., Girolami, M. & Sejnowski, T. J. 1999*b* Independent component analysis using an extended infomax algorithm for mixed sub-gaussian and super-gaussian sources. *Neural Comput.* **11**, 417–441.

Linsker, R. 1992 Local synaptic learning rules suffice to maximise mutual information in a linear network. *Neural Comput.* **4**, 691–702.

McKeown, M. J., Makeig, S., Brown, G. G., Jung, T.-P., Kindermann, S. S., Bell, A. J. & Sejnowski, T. J. 1998 Analysis of fMRI data by blind separation into independent spatial components. *Hum. Brain Mapp.* **6**, 160–188.

Makeig, S. 1993 Event-related dynamics of the EEG spectrum and effects of exposure to tones. *Electroencephalogr. Clin. Neurophysiol.* **86**, 283–293.

Makeig, S., Bell, A. J., Jung, T.-P. & Sejnowski, T. J. 1996 Independent component analysis of electroencephalographic data. In *Advances in neural information processing systems*, vol. 8 (ed. D. Touretzky, M. Mozer & M. Hasselmo), pp. 145–151. Cambridge, MA: MIT Press.

Makeig, S., Jung, T.-P., Ghahremani, D., Bell, A. J. & Sejnowski, T. J. 1997 Blind separation of auditory event-related brain responses into independent components. *Proc. Natl Acad. Sci. USA* **94**, 10 979–10 984.

Makeig, S., Jung, T.-P. & Sejnowski, T. J. 1998 Multiple coherent oscillatory components of human electroencephalogram (EEG) are differentially modulated by cognitive events. *Soc. Neurosci. Abstr.* **24**, 507.

Makeig, S., Westerfield, M., Jung, T.-P., Covington, J., Townsend, J., Sejnowski, T. J. & Courchesne, E. 1999 Independent components of the late positive event-related potential in a visual spatial attention task. *J. Neurosci.* **19**, 2665–2680.

Mangun, G. R. & Hillyard, S. A. 1991 Modulations of sensory-evoked brain potentials indicate changes in perceptual processing during visual–spatial priming. *J. Exp. Psychol. Hum. Percept. Perform.* **17**, 1057–1074.

Mesulam, M. M. 1981 A cortical network for directed attention and unilateral neglect. *Ann. Neurol.* **10**, 309–325.

Naatanen, R. & Picton, T. 1987 The N1 wave of the human electric and magnetic response to sound: a review and an analysis of the component structure. *Psychophysiology* **24**, 375–425.

Nadal, J.-P. & Parga, N. 1994 Non-linear neurons in the low noise limit: a factorial code maximises information transfer. *Network* **5**, 565–581.

Neville, H. J. & Lawson, D. 1987 Attention to central and peripheral visual space in a movement detection task: an event-related potential and behavioral study. I. Normal hearing adults. *Brain Res.* **405**, 253–267.

O'Donnell, B. F., Swearer, J. M., Smith, L. T., Hokama, H. & McCarley, R. W. 1997 A topographic study of ERPs elicited by visual feature discrimination. *Brain Topogr.* **10**, 133–143.

Saron, C. D. & Davidson, R. J. 1989 Visual evoked potential measures of interhemispheric transfer time in humans. *Behav. Neurosci.* **103**, 1115–1138.

Townsend, J. & Courchesne, E. 1994 Parietal damage and narrow 'spotlight' spatial attention. *J. Cogn. Neurosci.* **6**, 220–232.

Valdes-Sosa, M., Bobes, M. A., Rodriguez, V. & Pinilla, T. 1998 Switching attention without shifting the spotlight object-based attentional modulation of brain potentials. *J. Cogn. Neurosci.* **10**, 137–151.

Westerfield, M., Townsend, J., Makeig, S., Jung, T.-P., Sejnowski, T. J. & Courchesne, E. 1998 Independent components of the late positive event-related potential in a visual spatial attention task: normal and clinical subject differences. *Soc. Neurosci. Abstr.* **24**, 507.